MetaCaDI: A Meta-Learning Framework for Scalable Causal Discovery with Unknown Interventions

Hans Jarett Ong¹, Yoichi Chikahara², Tomoharu Iwata²

¹Nara Institute of Science and Technology, Nara, Japan ²NTT Communication Science Laboratories, Kyoto, Japan ong.hans_jarett.ol5@naist.ac.jp, chikahara.yoichi@gmail.com, tomoharu.iwata@ntt.com

Abstract

Uncovering the underlying causal mechanisms of complex real-world systems remains a significant challenge, as these systems often entail high data collection costs and involve unknown interventions. We introduce MetaCaDI, the first framework to cast the joint discovery of a causal graph and unknown interventions as a meta-learning problem. Meta-CaDI is a Bayesian framework that learns a shared causal structure across multiple experiments and is optimized to rapidly adapt to new, few-shot intervention target prediction tasks. A key innovation is our model's analytical adaptation, which uses a closed-form solution to bypass expensive and potentially unstable gradient-based bilevel optimization. Extensive experiments on synthetic and complex gene expression data demonstrate that MetaCaDI significantly outperforms state-of-the-art methods. It excels at both causal graph recovery and identifying intervention targets from as few as 10 data instances, proving its robustness in data-scarce sce-

1 Introduction

A central goal of scientific inquiry for understanding complex real-world systems is to move beyond mere correlation and uncover the underlying causal mechanisms. To achieve this goal, scientists typically rely on **interventional data**, obtained by performing an experimental intervention on specific variables. Since intervening the values of variables changes the distribution of their downstream variables (Eberhardt, Glymour, and Scheines 2005), comparing data with and without an intervention reveals both the presence and the direction of causal relationships between variables.

Scientific experiments often produce a collection of interventional datasets, each generated by intervening on different variables. Every such intervention acts as a clue to understand the cause-effect relationships. By assembling these "puzzle pieces", one can construct a single, comprehensive map of cause-effect relationships, typically formalized as a graph structure known as a *causal graph*.

When facing complex real-world systems, however, this endeavor faces two significant challenges. The first is the **scarcity of interventional data**: performing interventions on such systems is often costly and time-consuming, which severely limits the sample size available for each experiment and hinders reliable statistical inference. The second chal-

lenge is that the true intervention targets are often un**known** due to the difficulty of precisely intervening on the variables of interest in highly complex and interconnected systems. For example, widely used genome-editing tools like CRISPR/Cas9 can cause mutations in the unintended genes located near the target loci — a phenomenon known as off-target effects (Zhang et al. 2015). Identifying these unknown targets is a critical scientific goal in itself, crucial for diagnosing sources of change in a system like brain lesions (Siddigi et al. 2022) or fault detection in cloud computing systems (Varici et al. 2022). These challenges create an impasse: determining the causal direction from a pairwise comparison of interventional datasets requires knowledge of the intervention targets (Eaton and Murphy 2007), yet accurately inferring those targets needs a sufficient sample size for each dataset that is often unattainable in practice.

To overcome this impasse, we address the problem of few-shot joint inference: we aim to predict intervention targets for a small dataset to accurately infer the causal graph structure that is shared across all datasets; these datasets can include *observational datasets* (i.e., datasets with no interventions). We tackle this few-shot setting by taking a metalearning approach designed to learn an inference model that can rapidly adapt to new intervention target prediction tasks by extracting the task-shared causal graph knowledge.

To this end, we propose **MetaCaDI** (*Meta*-Learning for *Ca*usal *D*iscovery with Unknown *I*nterventions), a Bayesian framework that performs joint inference of the posterior distributions over the shared causal graph and the unknown intervention targets. By quantifying inference uncertainty with posterior probabilities, MetaCaDI offers reliable inference, even in data-scarce settings. Crucially, by framing this as a meta-learning problem, MetaCaDI is designed to rapidly adapt to new, individual datasets, a key advantage over traditional multitask approaches that require retraining on the entire collection of data. Our contributions are threefold:

- This work is the first to formalize the joint inference of a causal graph and unknown intervention targets as a meta-learning problem (Section 3). By framing the inference from each dataset as a distinct meta-learning *task*, our model extracts the *task-shared* knowledge of the causal graph structure and then leverages it to improve the performance of inferring *task-specific* intervention targets.
- To tackle this meta-learning problem, we establish a vari-

ational inference framework that infers posterior distributions over the shared causal graph and different intervention targets (Section 4). To effectively tune the task-specific parameters for each dataset, we formulate a likelihood model that admits a closed-form, analytical solution. This formulation eliminates the need for computationally demanding gradient-based optimization, as required by standard meta-learning methods (Finn, Abbeel, and Levine 2017), and enables high performance (Snell, Swersky, and Zemel 2017; Bertinetto et al. 2018).

• Through extensive experiments on synthetic and gene expression simulation datasets, we demonstrate that Meta-CaDI outperforms existing methods in recovering both the causal graph structure and the intervention targets, even in the challenging, small-sample setting.

2 Preliminaries

2.1 Causal Discovery from Observational and Interventional Data

We model the data-generating process over variables $\mathcal{X} = \{X_1, \dots, X_d\}$ using a **Structural Causal Model (SCM)** (Pearl 2009). Formally, an SCM defines a *structural equation*, which determines the values of each variable X_i $(j \in \{1, \dots, d\})$ as the output of a deterministic function f_i :

$$X_i = f_i(PA(X_i), E_i),$$

where $\operatorname{PA}(X_i) \subseteq \mathcal{X} \backslash X_i$ is a variable subset called the *parents* of X_i , and E_i is an exogenous variable (e.g., noise). **Causal graph** \mathcal{G} is defined as a graph that contains directed edge $X_j \to X_i$ if and only if $X_j \in \operatorname{PA}(X_i)$. In this paper, we make the two standard assumptions that \mathcal{G} is a directed acyclic graph (DAG) and that $E_i \perp E_j$ holds for any $i \neq j$; the latter, known as *causal sufficiency*, requires that there are no unobserved common causes (i.e., confounders).

Even under these assumptions, from observational data alone, a causal graph can only be identified up to its *Markov Equivalence Class (MEC)*—a set of causal graphs that encode the same conditional independence relations. To uniquely identify the causal graph structure, we assume the data follows an **Additive Noise Model (ANM)** (Hoyer et al. 2008), a widely-used identifiable SCM class with structural equation $X_i = f_i(\text{PA}(X_i)) + E_i$. This restricted functional form leads to distributional asymmetry between $X_i \to X_j$ and $X_i \leftarrow X_j$, theoretically guaranteeing the identifiability in the infinite-sample regime (Peters et al. 2014).

From finite-sample observational data, however, the inference can be unreliable, particularly when the sample size is small, and the distributional asymmetries used for causal graph inference are perturbed by the data sampling noise. A more robust source of inference comes from **interventional data**, collected by performing an intervention on the variable(s) in \mathcal{X} . An intervention on X_i alters its structural equation, changing the distribution of X_i and its descendants but not its ancestors. This allows for the disambiguation of causal directions that are otherwise indistinguishable, narrowing the set of possible graphs from an MEC to an Interventional MEC (I-MEC) (Eberhardt and Scheines 2007).

Method	Continuous Optimization	Uncertainty Quantification	Few-Shot Capability
JCI-PC	×	×	×
UT-IGSP	×	×	×
DCDI-G	\checkmark	×	×
BaCaDI	\checkmark	\checkmark	×
MetaCaDI (Ours)	\checkmark	\checkmark	\checkmark

Table 1: A comparison of causal discovery methods for interventional data. Our method, MetaCaDI, is the first to formalize the problem using a meta-learning paradigm, enabling rapid adaptation to unseen experimental settings.

2.2 Existing Approaches and Motivation

Several methods leverage collections of interventional datasets for causal discovery, as summarized in Table 1. Early methods such as **JCI-PC** (Mooij, Magliacane, and Claassen 2020) and **UT-IGSP** (Squires, Wang, and Uhler 2020), which take *constraint-based* and *score-based* approaches, respectively, suffer from scalability issues as the number of variables *d* increases. **DCDI-G** (Brouillard et al. 2020) addresses this limitation using continuous optimization. However, all these methods provide only a single point estimate of the causal graph and cannot quantify the uncertainty inherent in small datasets, where multiple causal graph structures might be equally plausible.

A principled way to capture this uncertainty is through Bayesian inference (Eaton and Murphy 2007). The stateof-the-art Bayesian approach, BaCaDI (Hägele et al. 2023), frames the problem as multitask learning, where it jointly infers a shared causal graph and all intervention targets across the training datasets. However, such a multitask learning approach has two critical shortcomings. First, accurately predicting intervention targets becomes challenging in the presence of sample size imbalance across datasets. This is because multitask learning is typically designed to optimize average performance across all tasks, often at the expense of underperforming on low-resource datasets. This drawback is problematic, as sample size imbalance is common due to the differences in data collection costs. For example, although detecting brain lesions under the sample size imbalance between patients and healthy controls is essential (Siddiqi et al. 2022; Bergmann and Hartwigsen 2021), achieving high performance becomes challenging for multitask learning approaches. Second, the multitask learning approach is ill-suited for real-time applications where data arrives sequentially. To illustrate this, consider a cloud computing system in which an engineer aims to quickly identify system faults via intervention target prediction (Varici et al. 2022; Mariani et al. 2018). Since multitask models require access to the full collection of datasets during the training phase, diagnosing a new fault from the newly arrived data would necessitate retraining the entire model from scratch, making the process too slow for real-time responsiveness.

These limitations highlight the need for a framework that can rapidly adapt to unseen and possibly small datasets without full-retraining, motivating a **meta-learning** approach.

3 Meta-Learning for Causal Discovery

3.1 Problem Setup

This section presents the meta-learning problem setup for causal discovery. Our meta-learning setup involves interventional data and stands in sharp contrast to existing meta-learning-based methods, which focus solely on observational data (Dhir et al. 2024; Wu, Shi, and Wang 2024).

As illustrated in Figure 1, we infer the causal graph structure shared across all datasets, as well as distinct intervention targets in each dataset. During the **meta-training phase**, we are given a collection of inference tasks $t=1,\ldots,T$, associated with *meta-training datasets* $\mathcal{D}_{\text{train}}=\{D_1,\ldots,D_T\}$. Each dataset D_t is a set of N_t i.i.d. observations of $\mathbf{X}=[X_1,\ldots,X_d]^\top$, given as $D_t=\{\mathbf{x}_n^t\}_{n=1}^{N_t} \overset{i.i.d.}{\sim} \mathbf{P}^{(t)}(\mathbf{X})$, where $\mathbf{x}_n^t \in \mathbb{R}^d$ $(n \in \{1,\ldots,N_t\})$ is an observation drawn from joint distribution $\mathbf{P}^{(t)}(\mathbf{X})$. We assume that $\mathbf{P}^{(t)}(\mathbf{X})$ is induced by performing a (hard or soft) intervention on a distinct variable subset in \mathbf{X} for task t, indicating that each dataset D_t is generated from a distinct experiment on the same system governed by a shared causal graph.

Based on this assumption, we consider the two inference targets. One is shared causal DAG adjacency matrix $\mathbf{A} \in \{0,1\}^{d \times d}$, which takes $A_{i,j} = 1$ if $X_i \to X_j$ in shared causal graph \mathcal{G} ; otherwise, $A_{i,j} = 0$. The other is binary intervention target vector $\mathbf{m}_t \in \{0,1\}^d$, which takes $m_{t,i} = 1$ if and only if the i-th variable X_i in X is experimentally manipulated; otherwise, $m_{t,i} = 0$. To enable the inference of \mathbf{m}_t in few-shot settings, we adapt a standard meta-learning strategy that randomly splits each meta-training dataset D_t into two disjoint subsets: a **support set** D_t^s and a **query set** D_t^q (illustrated by the green and red data instances in Figure 1). The support set, given as a small data subset, is used to mimic the few-shot setting, whereas the query set is the remaining data used to evaluate the quality of the task adaptation under such few-shot settings via a loss function.

During the **meta-test phase**, we aim to improve the inference performance by fine-tuning the trained joint inference model using a (possibly new and previously unseen) small dataset, called a *meta-test dataset* $D'_{t'}$.

3.2 Meta-Learning Strategy for Effective Posterior Inference

Our high-level objective is to infer the joint posterior distribution over the shared graph **A** and distinct intervention targets $\{m_t\}$ from the full collection of datasets $\mathcal{D}_{\mathcal{T}} = \{\mathcal{D}_{\text{train}}, \mathcal{D}'_{t'}\}$ in tasks $\mathcal{T} = \{1, \dots, T, t'\}$:

$$P(\mathbf{A}, \{\mathbf{m}_t\}_{t \in \mathcal{T}} | \mathcal{D}_{\mathcal{T}}) = P(\{\mathbf{m}_t\}_{t \in \mathcal{T}} | \mathbf{A}, \mathcal{D}_{\mathcal{T}}) P(\mathbf{A} | \mathcal{D}_{\mathcal{T}}).$$

Since this posterior is intractable, we approximate it with a variational distribution $P_{\Upsilon,\Phi}$ parameterized by *task-specific* parameters Υ and *task-shared parameters* Φ .

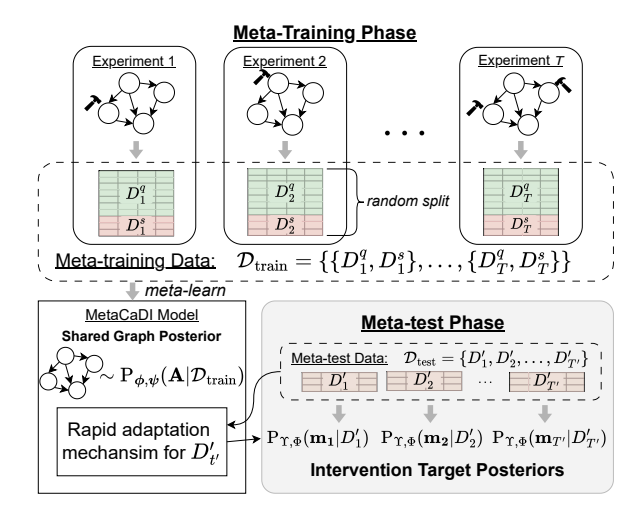


Figure 1: Our meta-learning setup. **Meta-training Phase**: Given a collection of datasets $\mathcal{D}_{\text{train}} = \{D_1, \dots, D_T\}$, MetaCaDI infers shared causal DAG adjacency matrix **A** from $\mathcal{D}_{\text{train}}$, as well as intervention target m_t for each D_t . **Meta-test Phase**: Using a new, small dataset $D'_{t'}$, MetaCaDI performs fine-tuning to infer its specific intervention targets.

Separating the parameters into such two sets is central to our meta-learning formulation. The shared components in a system, such as the causal graph structure, are captured by the task-shared parameters Φ whereas the task-specific components, such as the intervention targets, are represented by the task-specific parameters Υ . Consequently, conditioned on Φ , the specifics of each task can be treated as independent events. This consequence justifies our two modeling assumptions. First, intervention targets for two tasks t=a,b ($a\neq b$) are conditionally independent: $\mathbf{m}_a \perp \mathbf{m}_b \mid \Phi$. Second, since Φ is designed to act as a sufficient statistic that distills all generalizable knowledge from meta-training datasets $\mathcal{D}_{\text{train}}$, intervention targets for meta-test task t' are conditionally independent of $\mathcal{D}_{\text{train}}$: $\mathbf{m}_{t'} \perp \mathcal{D}_{\text{train}} \mid \Phi$. These assumptions yield the factorized variational formulation:

$$P(\mathbf{A}, \{\mathbf{m}_t\}_{t \in \mathcal{T}} \mid \mathcal{D}_{\mathcal{T}})$$

$$\approx P_{\Upsilon, \Phi}(\mathbf{A} \mid \mathcal{D}_{\mathcal{T}}) \prod_{t \in \mathcal{T}} P_{\Upsilon, \Phi}(\mathbf{m}_t \mid \mathbf{A}, D_t).$$
(1)

To learn the task-specific and task-shared parameters Υ and Φ , we solve a bi-level optimization problem where the inner loop adapts the task-specific parameters Υ to each distinct task t, and the outer loop optimizes the task-shared parameters Φ . Unlike standard meta-learning methods like MAML (Finn, Abbeel, and Levine 2017), we avoid using computationally expensive gradient-based optimization for the inner loop by designing our inference model to admit a closed-form, analytical solution to enable more efficient and stable task adaptation.

Remark 3.1 (**Identifiability**). When considering the infinite-sample regime where the posterior is dominated by likelihood, the existing identification results for non-Bayesian

¹A hard intervention on X_i replaces its structural equation with a constant, whereas a soft one modifies its structural equation while keeping its dependence on the values of its parents (Pearl 2009).

²Here we consider a single meta-test dataset $D'_{t'}$ for simplicity, but our method can be easily extended to multiple meta-test datasets $\mathcal{D}_{\text{test}} = \{D'_{t'}\}_{t'=1}^{T'}$.

methods (e.g., Brouillard et al. (2020)) can be applied to conclude that both \mathbf{A} and \mathbf{m}_t are identifiable under the ANM assumption in Section 2.1. In some exceptional cases (e.g., linear Gaussian ANMs), the causal graph can be identified only up to the I-MEC (Tian and Pearl 2001).

4 Proposed Method

This section presents **MetaCaDI**, a meta-learning framework for causal discovery with unknown intervention.

4.1 Variational Model Components

From datasets $\mathcal{D}_{\mathcal{T}} = \{\mathcal{D}_{\text{train}}, D'_{t'}\}$, MetaCaDI learns the variational distributions over shared causal DAG adjacency matrix \mathbf{A} and distinct intervention targets \mathbf{m}_t in task $t \in \mathcal{T}$. Below we present the model formulations for variational distributions $P_{\Upsilon,\Phi}(\mathbf{A} \mid \mathcal{D}_{\mathcal{T}})$ and $P_{\Upsilon,\Phi}(\mathbf{m}_t \mid \mathbf{A}, D_t)$ in Eq. (1), along with the likelihood model.

Differentiable Causal DAG Sampler We model the variational distribution $P_{\Phi}(\mathbf{A} \mid \mathcal{D}_{\mathcal{T}})$ by adopting the Differentiable Probabilistic DAG sampler (DP-DAG) (Charpentier, Kibler, and Günnemann 2022).

The benefits of employing the DP-DAG sampler are twofold. First, it guarantees the acyclicity of the sampled graphs, thereby aligning our inference procedure with theoretical identifiability conditions. To achieve this, it draws adjacency matrix $\mathbf{A} \in \{0,1\}^{d \times d}$ by sampling a strictly upper-triangular matrix $\mathbf{U} \in \{0,1\}^{d \times d}$ and a permutation matrix $\mathbf{\Pi} \in \{0,1\}^{d \times d}$ representing the node ordering, and then constructing the adjacency matrix using the classical DAG decomposition formula $\mathbf{A} = \mathbf{\Pi}^{\top} \mathbf{U} \mathbf{\Pi}$. Second, the sampler approximately computes the gradients of the sampling operations for these discrete matrices, thus enabling the use of recent advances in gradient-based inference. During backpropagation, it approximates the gradients using the continuous relaxations, $\tilde{\mathbf{U}} \in \mathbb{R}^{d \times d}$ and $\tilde{\mathbf{\Pi}} \in \mathbb{R}^{d \times d}$, which are sampled using the Gumbel-Softmax distribution (Jang, Gu. and Poole 2016; Maddison, Mnih, and Teh 2016) and the Gumbel-Top-k trick (Kool, van Hoof, and Welling 2020), respectively. We treat the parameters of these distributions, denoted by ϕ and ψ , as task-shared parameters Φ .

Differentiable Intervention Target Predictor Analogous to the variational distribution over causal DAGs, we model $P_{\Upsilon,\Phi}(\pmb{m}_t \mid \mathbf{A}, D_t)$ using a differentiable sampler. To approximate the gradient, we use a continuous relaxation of the binary intervention target vector $\pmb{m}_t \in \{0,1\}^d$, denoted by $\tilde{\pmb{m}}_t \in \mathbb{R}^d$, which is sampled from a Gumbel-Softmax distribution parameterized by a logit vector $\pmb{\zeta}^t \in \mathbb{R}^d$.

However, learning this logit vector is challenging: while predicting which variables are intervened upon in task t' ideally requires comparison with the observational data distribution, this comparison is infeasible in our setting, as the intervention targets are unknown in all datasets.

As we will describe in Section 4.2, we address this challenge not by comparing datasets but by comparing the *predicted* values of the variables with and without interventions. We obtain these predicted values using the likelihood model.

Likelihood Model Based on the ANM assumption, we formulate the structural equation of each variable as a sum of the observational and interventional mechanisms.

For each variable $X_i \in X$ in task t, we represent these two mechanisms by parameterizing two functions f_i and f_i^1 as the multi-layer perceptrons (MLPs) with parameters $\Theta_{\rm obs}$ and $\Theta_{\rm int}$, respectively. To represent their inputs, we use the i-th column of DAG adjacency matrix ${\bf A}$, denoted by ${\bf A}_i \in \{0,1\}^d$, as a binary mask vector that selects the parents of X_i . This yields the following parameterization of the structural equation:

$$X_{i} = (1 - m_{t,i}) \cdot f_{i}(\mathbf{A}_{i} \circ \mathbf{X}; \mathbf{\Theta}_{\text{obs}})$$

$$+ m_{t,i} \cdot f_{i}^{\text{I}}(\mathbf{A}_{i} \circ \mathbf{X}; \mathbf{\Theta}_{\text{int}}) + \epsilon_{i}, \quad (2)$$

where $\epsilon_i \sim \mathcal{N}(0,1)$ is standard Gaussian noise, and \circ denotes the Hadamard product. Here, the binary indicator $m_{t,j}$ in sampled vector \mathbf{m}_t acts as a switch between the observational mechanism f_i and the interventional mechanism f_i .

4.2 Modeling for Efficient Parameter Learning

Feature Design for Intervention Target Prediction Our modeling strategy for learning the intervention target predictor is not to learn its parameters but to train a neural network that outputs those parameters. Formally, we train the following neural network g_{η} (with parameters η) that outputs the logit parameters ζ^t of the Gumbel-Softmax distribution:

$$\boldsymbol{\zeta}^t = g_{\boldsymbol{\eta}}(\boldsymbol{F}_t). \tag{3}$$

where F_t is a feature vector, which we design to capture the information needed to predict the intervention targets m_t .

The advantages of this modeling strategy are twofold. First, by leveraging the dependence of input feature F_t on distinct task t, we can treat the parameters η as task-shared parameters, thus reducing the number of task-specific parameters Υ , which need to be trained on small support sets. Second, it can well specify helpful features for predicting intervention target m_t by including them in input feature F_t .

To design this input feature vector, we take three steps. First, we obtain the predicted variable values by applying the observational and interventional mechanisms in (2) to each data instance x_n^s in support set D_t^s :

$$\hat{\mathbf{x}}_{\text{obs }n}^s = f_i(\mathbf{A}_i \circ \mathbf{x}_n^s; \mathbf{\Theta}_{\text{obs}}) \text{ and } \hat{\mathbf{x}}_{\text{int }n}^s = f_i^{\text{I}}(\mathbf{A}_i \circ \mathbf{x}_n^s; \mathbf{\Theta}_{\text{int}}).$$

By concatenating these vectors in a row-wise manner, we obtain the two $N_t^s \times d$ matrices $\hat{\mathbf{X}}_{\mathrm{obs}}^s$ and $\hat{\mathbf{X}}_{\mathrm{int}}^s$, whose n-th row vectors are $\hat{\boldsymbol{x}}_{\mathrm{obs},n}^s$ and $\hat{\boldsymbol{x}}_{\mathrm{int},n}^s$, respectively.

Second, using the matrices $\hat{\mathbf{X}}_{\text{obs}}^s$ and $\hat{\mathbf{X}}_{\text{int}}^s$, we engineer a feature matrix, $\mathbf{C}_t \in \mathbb{R}^{N_t^s \times 9d}$ by concatenating the following nine $N_t^s \times d$ matrices in a column-wise manner:

$$\mathbf{C}_t = \begin{bmatrix} D_t^s, \hat{\mathbf{X}}_{\text{obs}}^s, D_t^s - \hat{\mathbf{X}}_{\text{obs}}^s, (D_t^s - \hat{\mathbf{X}}_{\text{obs}}^s)^2, \\ \hat{\mathbf{X}}_{\text{int}}^s, D_t^s - \hat{\mathbf{X}}_{\text{int}}^s, (D_t^s - \hat{\mathbf{X}}_{\text{int}}^s)^2, \boldsymbol{\mu}(D_t^s), \boldsymbol{\sigma}(D_t^s) \end{bmatrix},$$

where $\mu(D_t^s)$ and $\sigma(D_t^s)$ are the broadcasted column-wise mean and standard deviation of D_t^s , respectively.

Finally, we flatten the matrix C_t into a feature vector F_t so that the values of F_t are invariant to the order of data instances in the support set D_t^s . To achieve this, we formulate

the two permutation-invariant pooling layers based on the Deep Sets architecture (Zaheer et al. 2017). Using an MLP $h_{\varsigma}: \mathbb{R}^{9d} \to \mathbb{R}^k$ parameterized by task-shared parameters ς , these layers compute the **mean of embeddings** and the **embedding of the mean**:

$$\mathbf{z}_{\mathrm{ME}} = \frac{1}{N_t^s} \sum_{n=1}^{N_t^s} h_{\varsigma}(\boldsymbol{c}_{t,n}) \text{ and } \mathbf{z}_{\mathrm{EM}} = h_{\varsigma} \left(\frac{1}{N_t^s} \sum_{n=1}^{N_t^s} \boldsymbol{c}_{t,n} \right),$$

where embedding $c_{t,n}$ is the *n*-th row of C_t . By concatenating two vectors \mathbf{z}_{ME} and \mathbf{z}_{EM} , we obtain the final feature representation F_t as a vector of size 2k.

Closed-Form Solvers for Likelihood Fitting Since we have formulated an intervention target predictor using only task-shared parameters η and ς , the remaining task-dependent parameters are the MLP parameters for the interventional mechanism $f_i^{\rm I}$ in (2). However, as the number of MLP parameters is typically large, learning them only from a small dataset is challenging and prone to overfitting.

Our idea for overcoming this challenge is to reduce the number of task-specific parameters by treating only the last MLP layer of f_i^1 , denoted by w_i , as task-specific parameters. The preceding layers of the MLP act as a sophisticated feature extractor, which we treat as task-shared. This structure is defined as:

$$f_i^{\mathrm{I}}(\mathbf{A}_i \circ \mathbf{X}; \mathbf{\Theta}_{\mathrm{int}}) = \mathbf{w}_i^{\mathsf{T}} h_{\mathbf{\Theta}'_{\mathrm{int}}}(\mathbf{A}_i \circ \mathbf{X}), \tag{4}$$

where $h_{\Theta'_{\text{int}}}$ is the feature extraction part of the MLP (all layers except the last) with task-shared parameters $\Theta'_{\text{int}} = \Theta_{\text{int}} \setminus w_i$.

This formulation allows us to analytically obtain the optimal weights $\hat{\mathbf{w}}_i^{(t)}$ for each task by adapting to its support set D_t^s . We achieve this by solving a least-squares problem with an ℓ_2 regularizer (i.e., Ridge regression):

$$\min_{\mathbf{w}_{i}} \| (\mathbf{X}_{t}^{s})_{:,i} - \mathbf{H}_{i} \mathbf{w}_{i} \|_{2}^{2} + \lambda \| \mathbf{w}_{i} \|_{2}^{2},$$
 (5)

where $\lambda \geq 0$ is a regularization parameter. The target vector $(\mathbf{X}_t^s)_{:,i}$ is the i-th column of the support set data matrix $\mathbf{X}_t^s \in \mathbb{R}^{N_t^s \times d}$, containing the N_t^s observed values for variable X_i . The hidden feature matrix $\mathbf{H}_i \in \mathbb{R}^{N_t^s \times d_h}$ is generated by applying the feature extractor $h_{\mathbf{\Theta}_{\mathrm{int}}^t}$ to each of the N_t^s data samples in the support set, masked by the parents of X_i , where d_h is the dimension of the hidden representation. The vector of weights we aim to solve for is $\mathbf{w}_i \in \mathbb{R}^{d_h}$.

The regularized least-squares problem in Equation (5) has a well-known closed-form solution:

$$\hat{\boldsymbol{w}}_{i}^{(t)} = \left(\mathbf{H}_{i}^{\top}\mathbf{H}_{i} + \lambda \mathbf{I}\right)^{-1}\mathbf{H}_{i}^{\top}(\mathbf{X}_{t}^{s})_{:,i},\tag{6}$$

where I is the identity matrix. According to existing work on meta-learning (Snell, Swersky, and Zemel 2017; Bertinetto et al. 2018), such a closed-form solution enables fast and data-efficient task adaptation on D_t^s , bypassing the need for computationally demanding, iterative gradient-based optimization required by methods like MAML (Finn, Abbeel, and Levine 2017).

4.3 Training Objective

During the meta-training phase, MetaCaDI takes two steps. First, for each meta-training task t, it trains task-specific parameters $\Upsilon = \{w_1, \dots, w_d\}$ on the support set D_t^s based on Eq. (6). Then, using all meta-training datasets $\mathcal{D}_{\text{train}}$ and the trained task-specific parameters, it learns the task-shared parameters $\Phi = \{\phi, \psi, \eta, \varsigma, \Theta_{\text{obs}}, \Theta'_{\text{int}}\}$.

The objective of training task-shared parameters Φ lies in the posterior approximation. We aim to minimize the Kullback-Leibler (KL) divergence between the true and variational posteriors, which is equivalent to maximizing the Evidence Lower Bound (ELBO). Therefore, based on the negative ELBO, we consider the following expected loss:

$$\min_{\boldsymbol{\Phi}} \mathbb{E}_t[\mathbb{E}_{\mathbf{A}, \boldsymbol{m}_t}[-\log P(D_t^q \mid \mathbf{A}, \boldsymbol{m}_t)] + \Omega_{\Phi, t}],$$

where $-\log P(D_t^q \mid \mathbf{A}, \mathbf{m}_t)$ is the negative log-likelihood over the query set D_t^q for task t, and $\Omega_{\Phi,t}$ is a regularization term. We estimate the expectation over task t as an empirical average over meta-training tasks $t=1,\ldots,T$ and approximate the one over \mathbf{A} and \mathbf{m}_t using a single sample from our differentiable samplers presented in Section 4.1. Based on this approximation, we minimize the following weighted sum of four loss components:

$$\mathcal{L}(\Phi) = \frac{1}{T} \sum_{t=1}^{T} (\mathcal{L}_{R,t} + \lambda_I \mathcal{L}_{I,t} + \lambda_H \mathcal{L}_{H,t}) + \lambda_G \mathcal{L}_G, \quad (7)$$

where $\mathcal{L}_{R,t}$ is a **reconstruction loss**, which uses the mean squared error (MSE) to ensure the learned likelihood model accurately reproduces the data in the query set D_t^q ; $\mathcal{L}_{I,t}$ is an intervention sparsity regularizer, which applies an l^1 regularizer to logit vector $\boldsymbol{\zeta}^t$ to enforce the sparsity on the intervention target vector m_t ; $\mathcal{L}_{H,t}$ is a **residual independence** regularizer, which penalizes the dependence of residuals with the Hilbert-Schmidt Independence Criterion (HSIC) to enforce the causal sufficiency assumption in the ANMs; \mathcal{L}_C is a graph sparsity regularizer, which imposes sparsity on the edge presence probability in the causal graph using a KL divergence to align with the common nature of the causal graph structure in real-world systems; for encouraging the sparsity in the edge presence probability in the causal graph; $\lambda_I, \lambda_H, \lambda_G \geq 0$ are regularization parameters. We detail the full formulation of each loss component in Appendix B.

During the meta-test phase, we fine-tune task-specific parameters Υ on the meta-test dataset $D'_{t'}$ based on the closed-form solution in (6) to predict the intervention targets from $D'_{t'}$. If we have access to a large set of meta-test datasets, we can also fine-tune the task-shared parameters Φ using a similar objective in (7) to obtain a better approximation for Eq. (1). In our experiments, however, we do not perform this fine-tuning step, as it might perturb the learned task-shared parameters under the scarcity of meta-test datasets.

5 Experiments

5.1 Experimental Setup

We conduct a comprehensive evaluation of our proposed method, **MetaCaDI-Analytical**, against a suite of strong baselines on both synthetic and semi-synthetic datasets. We use these datasets because their ground-truth causal graph structures and intervention targets are known, which allows for a rigorous quantitative evaluation that is not feasible with most real-world datasets.

Baselines. We compare our method against four approaches: the constraint-based **JCI-PC** (Mooij, Magliacane, and Claassen 2020), the score-based **UT-IGSP** (Squires, Wang, and Uhler 2020), the continuous optimization-based **DCDI-G** (Brouillard et al. 2020), and the multitask Bayesian framework **BaCaDI** (Hägele et al. 2023). For an ablation study, we also include two variants of our method, both of which perform the gradient-based updates for task adaptation based on the MAML method (Finn, Abbeel, and Levine 2017) but differ in the updated parameters: **MetaCaDI-Intv-MAML** updates only the parameters of interventional mechanism f_i^l while **MetaCaDI-Full-MAML** updates all likelihood model parameters.

Datasets. We test all methods on synthetic and semisynthetic datasets. Synthetic data is generated from nonlinear ANMs whose nonlinear relationships are given by Gaussian Processes (GP). In contrast, we prepare semisynthetic data using a realistic gene expression simulator termed **SERGIO** (Dibaeinia and Sinha 2020), whose parameters are tuned on real gene expression data to represent the realistic noise. We detail the generation process for these datasets and their underlying causal graphs in Appendix A. For the meta-learning protocol, we consider T=20 metatraining tasks and generate each meta-training dataset of size $N_t = 110$, which are randomly split into a support set of size $N_t^s = 10$ and a query set of size $N_t^q = 100$. Crucially, for each of T' = 20 meta-test tasks, we consider a meta-test dataset that consists of only $N_{t'}^s = 10$ observations, simulating a challenging few-shot inference setup.

Evaluation Metrics. We evaluate performance on two fronts: causal graph discovery and intervention target prediction. For graph discovery, we use two standard metrics: the Expected Structural Hamming Distance (E-SHD), which measures the discrepancy between the true and inferred graphs, and the Expected Structural Intervention Distance (E-SID), which evaluates the quality of the inferred graph structure for estimating the interventional data distributions. For intervention target prediction, we use the Interventional AUROC (Intv-AUROC) and Interventional AUPRC (Intv-AUPRC). Full details for all metrics and experimental configurations are provided in Appendix A. To assess statistical significance in performance differences, we perform an independent two-sample Welch's t-test, which does not assume equal variance between groups.

5.2 Results

We perform 20 independent simulations³ and report the mean and standard deviation of each metric over these simulations. Figure 2 shows the results on both the SERGIO and

synthetic datasets. Performance is evaluated on causal structure discovery using E-SID and E-SHD, and on intervention target prediction using Intv-AUROC and Intv-AUPRC. Due to space limitation, we present the other metrics for graph discovery (AUROC and AUPRC) in Appendix G.1.

Intervention Target Prediction. Despite the challenging few-shot setting with only $N_{t'} = 10$ observations in metatest task t', our MetaCaDI-Analytical demonstrates a remarkable ability to identify intervention targets. This ability is most evident on the complex SERGIO dataset: our method achieves a mean Intv-AUROC of 0.740, significantly outperforming all baselines (p < 0.001 for all comparisons), and the highest mean Intv-AUPRC of 0.094, demonstrating the statistical significance (p < 0.005) over all methods except MetaCaDI-Intv-MAML (p = 0.067), the variant of our method. On the synthetic data, our MetaCaDI-Analytical again achieves the highest mean Intv-AUPRC of 0.351, with the improvement being statistically significant against four baselines (BaCaDI, DCDI-G, UT-IGSP, and MetaCaDI-Full-MAML with p < 0.001). Given that AUPRC explicitly accounts for false positives and is particularly informative under class-imbalanced settings, these improvements in Intv-AUPRC under sparse intervention settings underscore the effectiveness of our method in identifying rare interventions from a substantially small dataset.

Causal Graph Discovery. In the task of recovering the shared causal graph, our MetaCaDI-Analytical achieves better performance than BaCaDI and DCDI-G and proves to be highly competitive to JCI-PC and UT-IGSP. These results demonstrate that our method effectively infers the causal graph structure by aggregating the shared knowledge across datasets. Compared with the multitask Bayesian framework BaCaDI, our method achieves a far lower E-SID on both datasets. Given that our method significantly outperforms BaCaDI in intervention target prediction, this performance improvement indicates that our meta-learning approach effectively leverages the task-specific knowledge on the interventions in each task, thanks to our effective modeling strategies presented in Section 4.2.

Benefit of Analytical Adaptation. As an ablation study for investigating the advantage of our closed-form solvers for task adaptation, we compare our MetaCaDI-Analytical with its variants (MetaCaDI-Intv-MAML and MetaCaDI-Full-MAML), which do not use such solvers but instead perform gradient-based updates for task adaptation based on the MAML method (Finn, Abbeel, and Levine 2017).

As expected, in intervention target prediction, our method consistently outperforms both MAML variants on both datasets. This performance gap is statistically significant in most configurations; across the eight direct comparisons (2 MAML variants \times 2 datasets \times 2 metrics), MetaCaDI-Analytical's improvement was significant in five instances.⁴

³Due to computational challenges detailed in Appendix C, results for the BaCaDI baseline are averaged over a smaller number of simulations (16 for synthetic, 14 for SERGIO).

⁴These five configurations are: (i), (ii) Intv-AUROC and Intv-AUPRC on SERGIO against Full-MAML (p < 0.0001 and p = 0.003); (iii) Intv-AUROC on SERGIO against Intv-MAML (p = 0.0003); and (iv), (v) Intv-AUROC and Intv-AUPRC on Synthetic against Full-MAML (p < 0.0001).

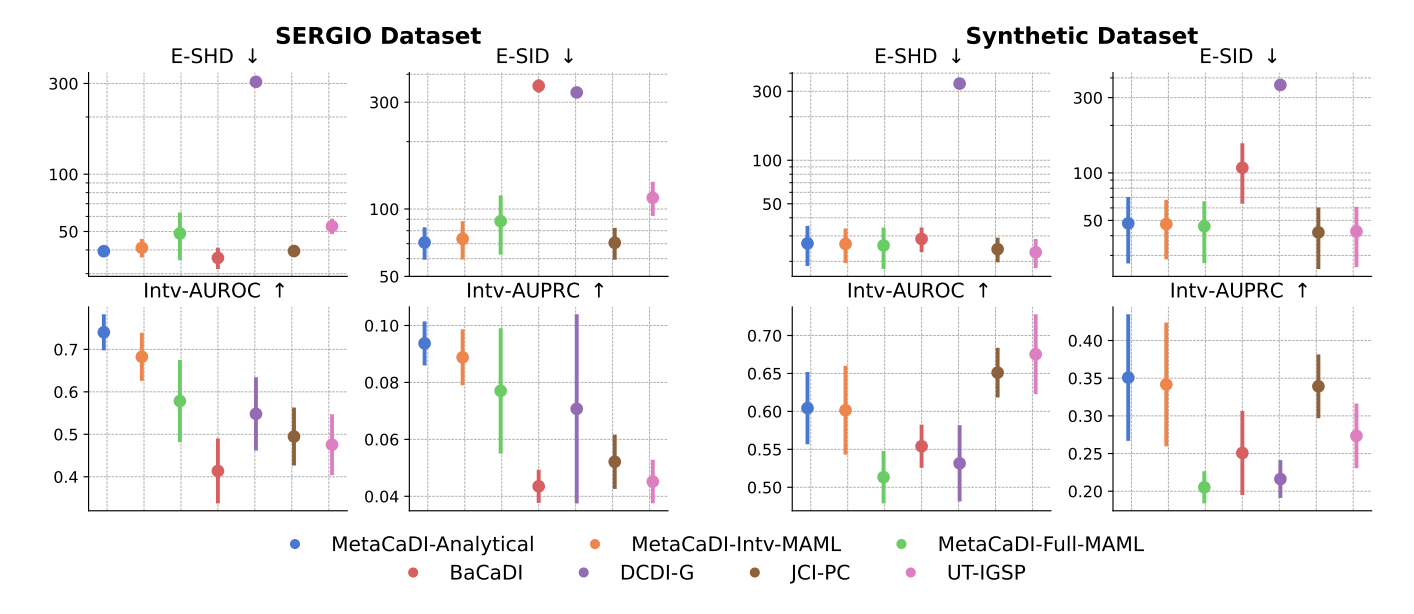


Figure 2: Performance comparison on the SERGIO and Synthetic datasets, with results averaged over 20 independent simulations³ per method. Error bars indicate the standard deviation. The y-axis for E-SID is on a logarithmic scale for easier comparison in the presence of outliers. ↓ and ↑ indicate "lower is better" and "higher is better", respectively.

We also observe a substantial improvement in computational speed, as detailed in the runtime comparison in Appendix G.2. Our method is over three times faster per training epoch than MetaCaDI-Full-MAML (e.g., 3.6 [sec.] vs. 11.3 [sec.] on SERGIO datasets). The efficiency benefit is even more pronounced in the task-adaptation step, where computing the closed-form solution is approximately 6.5 times faster than performing gradient-based updates (0.79 [sec.] vs. 5.0 [sec.] on average).

These results highlight a key finding: by designing a model that admits an analytical solution for fitting the task-specific parameters, we bypass the potentially unstable and computationally intensive gradient-based updates, enabling more robust and effective inference in few-shot setups.

Strong Performance under Challenging Scenarios. A key takeaway is MetaCaDI's robustness under realistic and challenging conditions. Its superior performance on the complex SERGIO dataset, which simulates noisy biological dynamics, suggests that the meta-learning objective fosters a model better equipped for real-world data than methods tuned to idealized synthetic processes.

It is worth noting that our method achieves strong performance in intervention target prediction under a more demanding evaluation protocol than baselines: MetaCaDI adapts the task-specific parameters to meta-test task t^\prime using only a single meta-test dataset $D_{t^\prime}^\prime$ with $N_{t^\prime}^s=10$ observations, whereas the baselines employ all $T^\prime=20$ meta-test datasets (See Appendix C for the details). Achieving competitive and often superior performance despite such challenging setup underscores the effectiveness of our modeling strategy for meta-learning and the versatility of our method in real-time applications where data arrives sequentially.

6 Future Work and Conclusion

Limitations and Future Work. Despite its strong performance, MetaCaDI currently relies on the ANM assumption, which may not fully capture the intricacies of complex systems. A promising direction for our future work is to enhance the flexibility by extending the likelihood model to encompass broader, identifiable SCM classes, such as postnonlinear models (PNLs) (Zhang and Hyvärinen 2009) or heteroscedastic noise models (HNMs) (Xu et al. 2022).

Conclusion. We proposed MetaCaDI, the first framework to formalize the joint discovery of a causal graph and unknown intervention targets as a meta-learning problem. By treating each interventional dataset as a distinct task, Meta-CaDI learns a posterior over the shared causal structure and unknown intervention targets. By developing an efficient model design for adapting to new, few-shot tasks, it addresses the practical challenge that requires to draw reliable conclusions from limited data where intervention effects are uncertain. Our proposed analytical adaptation method makes more effective and robust inference than the standard gradient-based meta-learning baselines. Comparison with existing methods tailored for interventional datasets shows that MetaCaDI outperforms them in both graph recovery and intervention target identification. Thus, our MetaCaDI represents a significant step towards building reliable causal inference tools for accelerating scientific discovery.

References

Bergmann, T.; and Hartwigsen, G. 2021. Inferring Causality from Noninvasive Brain Stimulation in Cognitive Neuroscience. *Journal of Cognitive Neuroscience*, 33: 195–225.

- Bertinetto, L.; Henriques, J. F.; Torr, P. H. S.; and Vedaldi, A. 2018. Meta-learning with differentiable closed-form solvers. *ArXiv*, abs/1805.08136.
- Brouillard, P.; Lachapelle, S.; Lacoste, A.; Lacoste-Julien, S.; and Drouin, A. 2020. Differentiable Causal Discovery from Interventional Data. In Larochelle, H.; Ranzato, M.; Hadsell, R.; Balcan, M.; and Lin, H., eds., *Advances in Neural Information Processing Systems*, volume 33, 21865–21877. Curran Associates, Inc.
- Charpentier, B.; Kibler, S.; and Günnemann, S. 2022. Differentiable DAG Sampling. *ArXiv*, abs/2203.08509.
- Dhir, A.; Ashman, M.; Requeima, J.; and van der Wilk, M. 2024. A Meta-Learning Approach to Bayesian Causal Discovery. *ArXiv*, abs/2412.16577.
- Dibaeinia, P.; and Sinha, S. 2020. SERGIO: A Single-Cell Expression Simulator Guided by Gene Regulatory Networks. *Cell Systems*, 11(3): 252–271.e11.
- Eaton, D.; and Murphy, K. 2007. Exact Bayesian structure learning from uncertain interventions. In Meila, M.; and Shen, X., eds., *Proceedings of the Eleventh International Conference on Artificial Intelligence and Statistics*, volume 2 of *Proceedings of Machine Learning Research*, 107–114. San Juan, Puerto Rico: PMLR.
- Eberhardt, F.; Glymour, C.; and Scheines, R. 2005. On the Number of Experiments Sufficient and in the Worst Case Necessary to Identify All Causal Relations Among N Variables. In *Conference on Uncertainty in Artificial Intelligence*.
- Eberhardt, F.; and Scheines, R. 2007. Interventions and Causal Inference. *Philosophy of Science*, 74(5): 981–995.
- Finn, C.; Abbeel, P.; and Levine, S. 2017. Model-Agnostic Meta-Learning for Fast Adaptation of Deep Networks. In *International Conference on Machine Learning*.
- Hägele, A.; Rothfuss, J.; Lorch, L.; Somnath, V. R.; Schölkopf, B.; and Krause, A. 2023. BaCaDI: Bayesian Causal Discovery with Unknown Interventions. In Ruiz, F.; Dy, J.; and van de Meent, J.-W., eds., *Proceedings of The 26th International Conference on Artificial Intelligence and Statistics*, volume 206 of *Proceedings of Machine Learning Research*, 1411–1436. PMLR.
- Hoyer, P.; Janzing, D.; Mooij, J. M.; Peters, J.; and Schölkopf, B. 2008. Nonlinear causal discovery with additive noise models. In Koller, D.; Schuurmans, D.; Bengio, Y.; and Bottou, L., eds., *Advances in Neural Information Processing Systems*, volume 21. Curran Associates, Inc.
- Jang, E.; Gu, S. S.; and Poole, B. 2016. Categorical Reparameterization with Gumbel-Softmax. *ArXiv*, abs/1611.01144.
- Kool, W.; van Hoof, H.; and Welling, M. 2020. Ancestral Gumbel-Top-k Sampling for Sampling Without Replacement. *Journal of Machine Learning Research*, 21(47): 1–36.
- Maddison, C. J.; Mnih, A.; and Teh, Y. W. 2016. The Concrete Distribution: A Continuous Relaxation of Discrete Random Variables. *ArXiv*, abs/1611.00712.
- Mariani, L.; Monni, C.; Pezzè, M.; Riganelli, O.; and Xin, R. 2018. Localizing Faults in Cloud Systems. 2018 IEEE 11th

- International Conference on Software Testing, Verification and Validation (ICST), 262–273.
- Mooij, J. M.; Magliacane, S.; and Claassen, T. 2020. Joint Causal Inference from Multiple Contexts. *Journal of Machine Learning Research*, 21(99): 1–108.
- Pearl, J. 2009. *Causality: Models, Reasoning and Inference*. USA: Cambridge University Press, 2nd edition. ISBN 052189560X.
- Peters, J.; Mooij, J. M.; Janzing, D.; and Schölkopf, B. 2014. Causal Discovery with Continuous Additive Noise Models. *Journal of Machine Learning Research*, 15(58): 2009–2053.
- Siddiqi, S.; Kording, K.; Parvizi, J.; and Fox, M. 2022. Causal mapping of human brain function. *Nature Reviews Neuroscience*, 23: 1–15.
- Snell, J.; Swersky, K.; and Zemel, R. 2017. Prototypical networks for few-shot learning. In *Proceedings of the 31st International Conference on Neural Information Processing Systems*, NIPS'17, 4080–4090. Red Hook, NY, USA: Curran Associates Inc. ISBN 9781510860964.
- Squires, C.; Wang, Y.; and Uhler, C. 2020. Permutation-Based Causal Structure Learning with Unknown Intervention Targets. In Peters, J.; and Sontag, D., eds., *Proceedings of the 36th Conference on Uncertainty in Artificial Intelligence (UAI)*, volume 124 of *Proceedings of Machine Learning Research*, 1039–1048. PMLR.
- Tian, J.; and Pearl, J. 2001. Causal Discovery from Changes. In *Proceedings of the 17th Conference in Uncertainty in Artificial Intelligence*, UAI '01, 512–521. San Francisco, CA, USA: Morgan Kaufmann Publishers Inc. ISBN 1558608001.
- Varici, B.; Shanmugam, K.; Sattigeri, P.; and Tajer, A. 2022. Intervention target estimation in the presence of latent variables. In Cussens, J.; and Zhang, K., eds., *Proceedings of the Thirty-Eighth Conference on Uncertainty in Artificial Intelligence*, volume 180 of *Proceedings of Machine Learning Research*, 2013–2023. PMLR.
- Wu, H.; Shi, W.; and Wang, M. 2024. Developing a novel causal inference algorithm for personalized biomedical causal graph learning using meta machine learning. *BMC Medical Informatics and Decision Making*, 24.
- Xu, S.; Mian, O. A.; Marx, A.; and Vreeken, J. 2022. Inferring cause and effect in the presence of heteroscedastic noise. In *International Conference on Machine Learning*, 24615–24630. PMLR.
- Zaheer, M.; Kottur, S.; Ravanbhakhsh, S.; Póczos, B.; Salakhutdinov, R.; and Smola, A. J. 2017. Deep Sets. In *Proceedings of the 31st International Conference on Neural Information Processing Systems*, NIPS'17, 3394–3404. Red Hook, NY, USA: Curran Associates Inc. ISBN 9781510860964.
- Zhang, K.; and Hyvärinen, A. 2009. On the identifiability of the post-nonlinear causal model. In *Proc. 25th Conference on Uncertainty in Artificial Intelligence (UAI2009)*.
- Zhang, X.-H.; Tee, L. Y.; Wang, X.-G.; Huang, Q.-S.; and Yang, S.-H. 2015. Off-target Effects in CRISPR/Cas9-mediated Genome Engineering. *Molecular Therapy Nucleic Acids*, 4: e264.